Space-Time Block Coding for Uplink Single-Carrier CDMA with Joint Detection in the Frequency Domain

François Horlin *Eduardo Lopez-Estraviz* *Liesbet Van der Perre*

Interuniversity Micro-Electronics Center (IMEC)
Wireless Research
Kapeldreef 75, B-3001 Leuven, Belgium

E-mail : francois.horlin@imec.be

Abstract—**Single-carrier code-division multiple access (SC-CDMA), also named cyclic-prefix CDMA in the literature, is a promising air interface for the uplink of the 4G cellular wireless communication systems. It enables the high capacity intrinsically offered by CDMA by making the equalization of the multipath channels and the mitigation of the resulting interference possible at a low complexity. This paper proposes a new air interface that combines SC-CDMA with space-time block coding (STBC) across multiple transmit antennas in order to make the link more robust. Contrary to existing air interfaces that perform the STBC at the chip level, making them only applicable to the downlink, the STBC is performed at the symbol level, making it also applicable to the uplink. In order to optimally detect the different antenna and user signals, a linear joint detector optimized according to the minimum mean square error (MMSE) criterion is designed. By exploiting the cyclic properties of the channel matrices, the complexity of the joint detector is significantly reduced. Furthermore, it is shown analytically that the inter-antenna interference is canceled out at the output of the first stage of the linear MMSE joint detector, consisting of a matched filter. By space-time coding the signal through two antennas at each transmit mobile terminal, a significant gain in signal-to-noise-ratio can be achieved. However, the spatial diversity gain of the proposed system is limited by the multi-user interference (MUI), that is increasing with the user load. Higher complexity non-linear receivers are needed to better compensate the MUI and still benefit from the spatial diversity at high user loads.**

I. Introduction

In order to meet the high data rate and quality-of-service (QoS) requirements of the future broadband cellular systems, it is now widely accepted that multiple antenna techniques should be used in combination to newly designed air interfaces.

Cellular systems of the third generation (3G) are based on the direct-sequence code-division multiple access (DS-CDMA) technology [1]. DS-CDMA enables a high system capacity and offers interesting networking abilities, like soft hand-over between two neighboring cells. However, the system suffers from inter-symbol interference (ISI) and multiuser interference (MUI) caused by multipath propagation, leading to a significant loss of performance in typical outdoor environments. For this reason, the spectral efficiency of 3G DS-CDMA communication systems is very low.

In order to enable the design of low complexity transceivers that can cope with multipath channels while still benefiting from the good properties of DS-CDMA, next generation cellular systems could combine the DS-CDMA accessing scheme with the single-carrier block transmission (SCBT), also known as single-carrier (SC) modulation with cyclic prefix [2], [3]. Similar to orthogonal frequency division multiplexing (OFDM), SCBT transforms a time dispersive channel into a set of parallel independent flat sub-channels that can be equalized at a low complexity. SCBT has been recognized as an interesting alternative to OFDM in the uplink, that could significantly reduce the terminal processing complexity (the inverse fast Fourier transform (IFFT) operator is moved to the receiver base station) as well as the constraints on the analog front-end (the peak-to-average power ratio (PAPR) is significantly reduced) [4]. When combining DS-CDMA with SCBT, the DS-CDMA signals are either spread within one block across the SC sub-channels, leading to single-carrier CDMA (SC-CDMA) [5], [6], or across the SCBT blocks, leading to single-carrier block-spread CDMA (SCBS-CDMA) [7], [8]. SC-CDMA and SCBS-CDMA can be seen as the SC counter-parts of multi-carrier CDMA (MC-CDMA) [9], [10] and multi-carrier block-spread CDMA (MCBS-CDMA) [11], [12], [13], respectively. When the channels are constant over the time (or at least over one symbol block duration), SCBS-CDMA preserves the orthogonality among the users, regardless of the underlying multipath pattern. Perfect user separation is first obtained through low complexity code correlation, and followed by the equalization of the propagation channel in the frequency domain [7], [8]. On the contrary, SC-CDMA does not preserve the orthogonality amongst the users in the presence of multipath propagation. In the downlink, a single-user detector is usually used, that consists of a chip equalizer to estimate the streams of chips by simple channel inversion in the frequency domain, and of a code correlator to separate the user signals [6]. In the uplink, however, advanced joint detection techniques have to be considered that jointly detect the user symbol blocks transmitted over different propagation channels. The complexity of the joint detector can still be significantly reduced by using the circulant properties of the channel matrices [5]. SCBS-CDMA entails a larger symbol latency than SC-CDMA, that makes it impractical in medium-to-high mobility cellular environments [14].

Multiple-input multiple-output (MIMO) systems, which deploy multiple antennas at both ends of the wireless link, explore the extra spatial dimension, besides the time, frequency, and code dimensions, to significantly increase the spectral efficiency, and to improve the link reliability relative to single antenna systems. In this context, space-time block coding (STBC) has recently gained a lot of attention as an effective transmit diversity technique to combat fading in wireless communications.

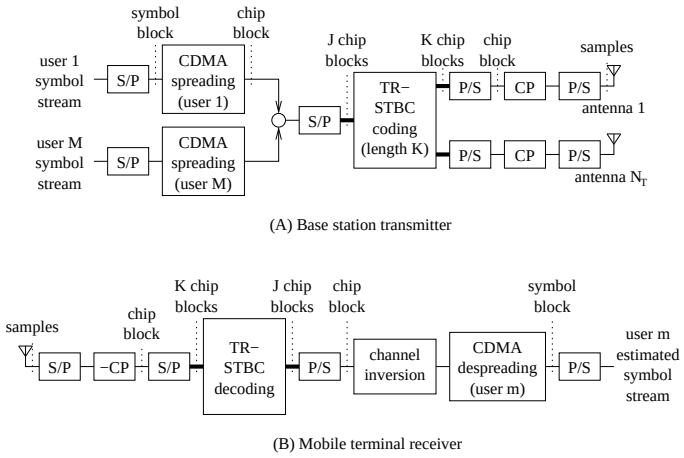

Fig. 1. Combination SC-CDMA and STBC in the downlink; STBC parameters: J: number of encoded chip blocks, K: code length, N_T: number of transmit antennas.

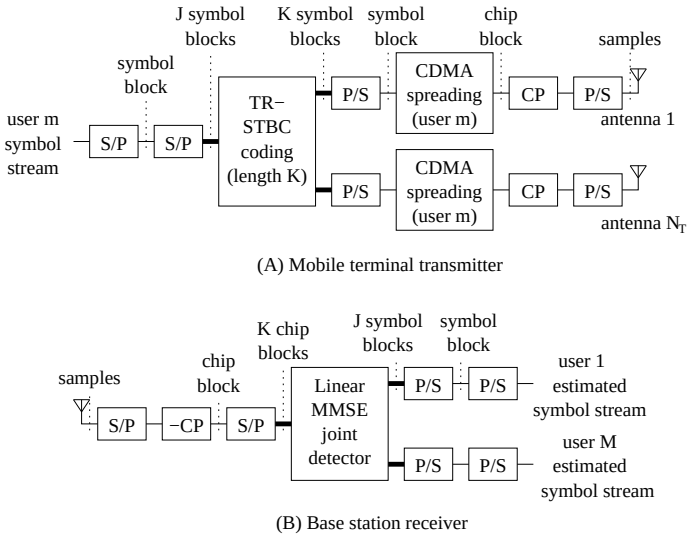

Fig. 2. Combination SC-CDMA and STBC in the uplink; STBC parameters: J: number of encoded symbol blocks, K: code length, N_T: number of transmit antennas.

Orthogonal space-time (ST) block codes for two transmit antennas have first been introduced in [15] and later generalized to an arbitrary number of transmit antennas in [16]. The ST codes are initially designed for frequency flat fading channels. Therefore, the time reversal (TR) STBC technique is proposed in [17] as an extension of [15] to frequency selective channels. These designs have remarkably simple maximum-likelihood (ML) decoding algorithms based on linear processing at the receiver. In specific cases of two or four transmit antennas, these diversity schemes provide full and three-quarters of the maximum possible transmission rate, respectively [18].

The combination of STBC with the SC-based air interfaces has only been addressed very recently. Papers [19] and [20] combine STBC with SCBS-CDMA. Since the SCBS-CDMA scheme is orthogonal in the users (both for uplink and downlink), deterministic ML user separation through low-complexity code matched filtering and ML ST multi-stream separation through linear decoding can be consecutively applied without any performance loss with respect to the optimal ML joint multi-user detector and ST block decoder. On the other hand, [21] and [22] apply STBC in the downlink of a SC-CDMA-based system (see the description in Figure 1). The TR STBC technique is applied at the chip level, on the signals resulting from the CDMA spreading, in order to improve the robustness of the estimation of the streams of chips at the receiver against channel fading. A cyclic-prefix (CP) is added at the transmitter before sending the signal through the channel, and removed at the receiver. The single-user detector, intuitively composed of the counter-part of each operation at the transmitter, first performs the STBC decoding and the inversion of the channels, followed by the CDMA user despreading. Paper [23] shows that the system illustrated in Figure 1 can hardly be applied to the uplink because its performance is limited by the MUI.

This paper combines STBC with SC-CDMA, considering the uplink of the communication system (see the description in Figure 2). Because the advanced joint detector required in the uplink does not rely on the preliminary estimation of the streams of chips, but instead, directly considers the joint estimation of the user symbols, the STBC scheme has to be applied at the symbol level, before the CDMA spreading, in order to improve the robustness of the estimation of the streams of symbols at the receiver against channel fading. At the receiver, a low complexity joint multi-user detector and ST block decoder, optimized according to the minimum mean square error (MMSE) criterion, is designed. A successive interference canceler (SIC), built based on the linear MMSE joint detector, is also considered. It is demonstrated that the proposed scheme preserves the orthogonality between the transmit antenna symbol streams and benefits from the spatial diversity offered by the use of multiple transmit antennas at the mobile terminals.

The paper is organized as follows. The transmitter model is presented in Section II. The STBC, CDMA spreading and single-carrier block transmission operations are successively detailed. A matrix model is defined in Section III, that relies on the circulant properties of the matrices resulting from the use of a cyclic prefix. The joint detector is designed in Section IV. Using a frequency domain representation, it is shown that the complexity of the receiver can be significantly reduced and that the inter-antenna interference can be totally canceled out, bringing the desired diversity gain. Finally the gain obtained by exploiting spatial and/or multipath diversity is quantified in Section V for outdoor channels.

In the sequel, we use single- and double-underlined letters for the vectors and matrices respectively. Matrix $\underline{\underline{I}}_N$ is the identity matrix of size N and matrix $\underline{\underline{0}}_{M\times N}$ is a matrix of zeros of size $M \times N$. The operators $(.)^*$, $(.)^T$ and $(.)^H$ denote the complex conjugate, transpose and conjugate transpose of a vector or a matrix respectively. The operator $\otimes$ is the Kronecker product between two vectors or matrices. We index the transmitted block sequence by i, and the STBC-coded block sequence and the chip block sequence by n.

II. Transmitter

The transmission scheme for the m-th user ($m = 1, \cdots, M$) is depicted in Figure 3. Each user sends its data through N_T transmit antennas. The information symbols, $d_{n_T}^m[i]$ ($n_T = 1, \cdots, N_T$), assumed independent with

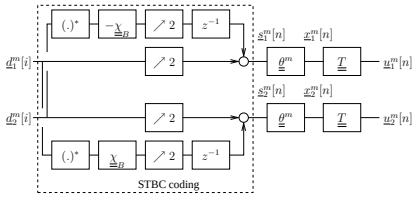

Fig. 3. Transmitter model ($N_T = 2$).

variance σ_d^2, are first serial-to-parallel converted into blocks of B symbols, leading to the block sequence, $\underline{d}_{n_T}^m[i] := [d_{n_T}^m[iB] \ldots d_{n_T}^m[(i+1)B-1]]^T$.

A. Space-time block coding

For conciseness, we limit ourself to the case of $N_T = 2$ transmit antennas and extend the STBC scheme proposed in [15], [17] to the uplink of a SC-CDMA-based communication system. However the developments can be extended to any number of antennas, by using the orthogonal coding designs proposed in [16].

The STBC technique is implemented by coding the two antenna streams across two time instants, as expressed in:

$$\begin{bmatrix} \underline{s}_1^m[n] \\ \underline{s}_2^m[n] \end{bmatrix} = \begin{bmatrix} \underline{d}_1^m[i] \\ \underline{d}_2^m[i] \end{bmatrix} \quad (1)$$

$$\begin{bmatrix} \underline{s}_1^m[n+1] \\ \underline{s}_2^m[n+1] \end{bmatrix} = \underline{\underline{\chi}} \cdot \begin{bmatrix} \underline{d}_1^m[i]^* \\ \underline{d}_2^m[i]^* \end{bmatrix} \quad (2)$$

where $i = \lfloor n/2 \rfloor$. The coding matrix $\underline{\underline{\chi}}$ is the result of the Kronecker product of the two submatrices $\underline{\underline{\chi}}_{N_T}$, that implements the simple Alamouti scheme across two antennas in flat fading channels [15], and $\underline{\underline{\chi}}_B$, that implements the additional time-reversal permutation needed for time-dispersive channels [17], as expressed in $\underline{\underline{\chi}} := \underline{\underline{\chi}}_{N_T} \otimes \underline{\underline{\chi}}_B$. They are defined as:

$$\underline{\underline{\chi}}_{N_T} := \begin{bmatrix} 0 & -1 \\ 1 & 0 \end{bmatrix} \quad (3)$$

$$\underline{\underline{\chi}}_B := \underline{\underline{F}}_B^T \cdot \underline{\underline{F}}_B \quad (4)$$

where $\underline{\underline{F}}_J$ is the size-J fast Fourier transform (FFT) matrix, given by:

$$\underline{\underline{F}}_J := \left[\frac{1}{\sqrt{J}} e^{-j2\pi \frac{pq}{J}} \right]_{p,q=0,\cdots,J-1}. \quad (5)$$

It is easy to verify that the transmitted block at time instant $n+1$ from one antenna is the time-reversed conjugate of the transmitted block at time instant n from the other antenna (with possible permutation and sign change). As we will show later, this property allows for deterministic transmit stream separation at the receiver, regardless of the underlying frequency selective channels.

B. CDMA spreading

As we have indicated in the introduction, SC-CDMA first performs classical DS-CDMA symbol spreading, followed by SCBT modulation, such that the information symbols are spread across the different SCBT sub-channels [5], [6].

With $Q = BN$ and N the spreading code length, the $Q \times B$ spreading matrix, $\underline{\underline{\theta}}^m$, that spreads the symbols across the subchannels, is defined as:

$$\underline{\underline{\theta}}^m := \underline{\underline{I}}_B \otimes \underline{a}^m, \quad (6)$$

with $\underline{a}^m := [a^m[0] \ldots a^m[N-1]]^T$ the m-th user's $N \times 1$ code vector. The blocks $\underline{x}_{n_T}^m[n]$ are obtained by multiplying the blocks $\underline{s}_{n_T}^m[n]$ with the $\underline{\underline{\theta}}^m$ spreading matrix:

$$\underline{x}_{n_T}^m[n] := \underline{\underline{\theta}}^m \cdot \underline{s}_{n_T}^m[n]. \quad (7)$$

C. Cyclic-prefix addition

Finally, the $K \times Q$ transmit matrix, $\underline{\underline{T}}$, adds some transmit redundancy to the time-domain chip blocks:

$$\underline{u}_{n_T}^m[n] := \underline{\underline{T}} \cdot \underline{x}_{n_T}^m[n]. \quad (8)$$

With $K = Q+L$, $\underline{\underline{T}} = \underline{\underline{T}}_{cp} := [\underline{\underline{I}}_{cp}^T, \underline{\underline{I}}_Q^T]^T$, where $\underline{\underline{I}}_{cp}$ consists of the last L rows of $\underline{\underline{I}}_Q$, $\underline{\underline{T}}$ adds redundancy in the form of a length-L cyclic prefix. The resulting transmitted chip block sequence, $\underline{u}_{n_T}^m[n]$, is parallel-to-serial converted into the scalar sequence, $[u_{n_T}^m[nK] \ldots u_{n_T}^m[(n+1)K-1]]^T := \underline{u}_{n_T}^m[n]$, and transmitted over the air at a rate $1/T_c$.

III. System model

A. Multipath propagation and blocking

After propagation through the different user channels, the signal is received at N_R receive antennas. Adopting a discrete-time baseband equivalent model, the chip-sampled received signal at antenna n_R ($n_R = 1, \cdots, N_R$), $v_{n_R}[n]$, is the superposition of channel-distorted versions of the MN_T transmitted user signals, which can be written as:

$$v_{n_R}[n] = \sum_{m=1}^{M} \sum_{n_T=1}^{N_T} \sum_{l=0}^{L^m} h_{n_R,n_T}^m[l] u_{n_T}^m[n-l] + w_{n_R}[n]. \quad (9)$$

The additive white Gaussian noise (AWGN) at the base station antenna n_R, $w_{n_R}[n]$, has a variance equal to σ_w^2. The channel $h_{n_R,n_T}^m[l]$ of order L^m models the frequency-selective multipath propagation between the m-th user antenna n_T and the base station antenna n_R, and includes the effect of transmit/receive filters and the remaining asynchronism of the quasi-synchronous users. The maximum channel order L_{max}, that is $L_{max} = \max_m\{L^m\}$, can be well approximated by $L_{max} \approx \lfloor (\tau_{max,a} + \tau_{max,s})/T_c \rfloor + 1$, where $\tau_{max,a}$ is the maximum asynchronism between the nearest and the farthest user of the cell, and $\tau_{max,s}$ is the maximum excess delay within the given propagation environment. In the sequel, we assume that the CP length has been chosen such that $L \geq L_{max}$.

Assuming perfect time and frequency synchronization, the received sequence, $v_{n_R}[n]$, is serial-to-parallel converted into the block sequence, $\underline{v}_{n_R}[n] := [v_{n_R}[nK] \ldots v_{n_R}[(n+1)K-1]]^T$. From the scalar input/output relationship in (9), we can derive

the corresponding block input/output relationship:

$$\underline{v}_{n_R}[n] = \sum_{m=1}^{M}\sum_{n_T=1}^{N_T}(\underline{\underline{H}}^m_{n_R,n_T}[0]\cdot\underline{u}^m_{n_T}[n] + \underline{\underline{H}}^m_{n_R,n_T}[1]\cdot\underline{u}^m_{n_T}[n-1]) + \underline{w}_{n_R}[n], \quad (10)$$

where $\underline{w}_{n_R}[n] := [w_{n_R}[nK]\ldots w_{n_R}[(n+1)K-1]]^T$ is the corresponding noise block sequence, $\underline{\underline{H}}^m_{n_R,n_T}[0]$ is a $K\times K$ lower triangular Toeplitz matrix with entries $[\underline{\underline{H}}^m_{n_R,n_T}[0]]_{p,q} = h^m_{n_R,n_T}[p-q]$, and $\underline{\underline{H}}^m_{n_R,n_T}[1]$ is a $K\times K$ upper triangular Toeplitz matrix with entries $[\underline{\underline{H}}^m_{n_R,n_T}[1]]_{p,q} = h^m_{n_R,n_T}[K+p-q]$ (see e.g. [24] for a detailed derivation of the single-user case). The delay-dispersive nature of multipath propagation gives rise to so-called inter-block interference (IBI) between successive blocks, which is modeled by the second term in (10).

The $Q\times K$ receive matrix, $\underline{\underline{R}}$, removes the redundancy from the chip blocks, that is, $\underline{y}_{n_R}[n] := \underline{\underline{R}}\cdot\underline{v}_{n_R}[n]$. With $\underline{\underline{R}} = \underline{\underline{R}}_{cp} := [\underline{\underline{0}}_{Q\times L}, \underline{\underline{I}}_Q]$, $\underline{\underline{R}}$ again discards the length-L cyclic prefix. The purpose of the transmit $\underline{\underline{T}}$/receive $\underline{\underline{R}}$ pair is twofold. First, it allows for simple block-by-block processing by removing the IBI, that is, $\underline{\underline{R}}\cdot\underline{\underline{H}}^m_{n_R,n_T}[1]\cdot\underline{\underline{T}} = \underline{\underline{0}}$, provided the CP length to be at least the maximum channel order L_{max}. Second, it enables low-complexity frequency-domain processing by making the linear channel convolution appear circulant to the received block. This results in a simplified block input/output relationship in the time-domain:

$$\underline{y}_{n_R}[n] = \sum_{m=1}^{M}\sum_{n_T=1}^{N_T}\dot{\underline{\underline{H}}}^m_{n_R,n_T}\cdot\underline{x}^m_{n_T}[n] + \underline{z}_{n_R}[n], \quad (11)$$

where $\dot{\underline{\underline{H}}}^m_{n_R,n_T} = \underline{\underline{R}}\cdot\underline{\underline{H}}^m_{n_R,n_T}[0]\cdot\underline{\underline{T}}$ is a circulant channel matrix, and $\underline{z}_{n_R}[n] = \underline{\underline{R}}\cdot\underline{w}_{n_R}[n]$ is the corresponding noise block sequence.

B. Matrix model

In order to design the multi-user joint detector, a generalized matrix model of the system is necessary. We build first a matrix model that relates the STBC-coded symbols to the received samples at the different antennas, and extend it next to encompass the STBC coding.

The generalized input/output matrix model, that links the STBC-coded symbols to the received samples, is given by:

$$\underline{y}[n] = \underline{\underline{H}}\cdot\underline{\underline{\theta}}\cdot\underline{s}[n] + \underline{z}[n], \quad (12)$$

taking (7) into account. The vector of symbols is a vertical concatenation of the user and transmit antenna specific vectors of symbols ($N_T = 2$):

$$\underline{s}[n] := \left[\begin{array}{ccc}\underline{s}^1[n]^T & \cdots & \underline{s}^M[n]^T\end{array}\right]^T \text{ with} \quad (13)$$

$$\underline{s}^m[n] := \left[\begin{array}{ccc}\underline{s}^m_1[n]^T & \cdots & \underline{s}^m_{N_T}[n]^T\end{array}\right]^T \quad (14)$$

for $m = 1,\cdots,M$, and the received and noise vectors are a vertical concatenation of the receive antenna specific received and noise vectors:

$$\underline{y}[n] := \left[\begin{array}{ccc}\underline{y}_1[n]^T & \cdots & \underline{y}_{N_R}[n]^T\end{array}\right]^T \quad (15)$$

$$\underline{z}[n] := \left[\begin{array}{ccc}\underline{z}_1[n]^T & \cdots & \underline{z}_{N_R}[n]^T\end{array}\right]^T. \quad (16)$$

The channel matrix is equal to:

$$\underline{\underline{H}} := \left[\begin{array}{ccc}\underline{\underline{H}}^T_1 & \cdots & \underline{\underline{H}}^T_{N_R}\end{array}\right]^T \quad (17)$$

in which each matrix $\underline{\underline{H}}_{n_R}$ specific to the antenna n_R is composed of MN_T matrices specific to the user and transmit antennas, as defined in:

$$\underline{\underline{H}}_{n_R} := \left[\begin{array}{ccc}\underline{\underline{H}}^1_{n_R} & \cdots & \underline{\underline{H}}^M_{n_R}\end{array}\right] \text{ with} \quad (18)$$

$$\underline{\underline{H}}^m_{n_R} := \left[\begin{array}{ccc}\dot{\underline{\underline{H}}}^m_{n_R,1} & \cdots & \dot{\underline{\underline{H}}}^m_{n_R,N_T}\end{array}\right] \quad (19)$$

for $n_R = 1,\cdots,N_R$ and $m = 1,\cdots,M$, and the CDMA spreading matrix is equal to:

$$\underline{\underline{\theta}} := \left[\begin{array}{ccc}\underline{\underline{I}}_{N_T}\otimes\underline{\theta}^1 & \cdots & \underline{\underline{0}}_{N_TQ\times N_TB}\\ \vdots & \ddots & \vdots\\ \underline{\underline{0}}_{N_TQ\times N_TB} & \cdots & \underline{\underline{I}}_{N_T}\otimes\underline{\theta}^M\end{array}\right]. \quad (20)$$

The model (12) can be extended to the STBC input/output matrix model:

$$\underline{y}_{stbc}[i] = \underline{\underline{H}}_{stbc}\cdot\underline{\underline{\theta}}_{stbc}\cdot\underline{\underline{\chi}}_{stbc}\cdot\underline{d}[i] + \underline{z}_{stbc}[i], \quad (21)$$

taking (1) and (2) into account. The vector of symbols is also a vertical concatenation of the user and transmit antenna specific vectors of symbols ($N_T = 2$):

$$\underline{d}[i] := \left[\begin{array}{ccc}\underline{d}^1[i]^T & \cdots & \underline{d}^M[i]^T\end{array}\right]^T \text{ with} \quad (22)$$

$$\underline{d}^m[i] := \left[\begin{array}{ccc}\underline{d}^m_1[i]^T & \cdots & \underline{d}^m_{N_T}[i]^T\end{array}\right]^T \quad (23)$$

for $m = 1,\cdots,M$. The received and noise vectors are formed by stacking the vectors corresponding to the first time instant on top of the conjugate of the vectors corresponding to the second time instant:

$$\underline{y}_{stbc}[i] := \left[\begin{array}{c}\underline{y}[n]\\ \underline{y}[n+1]^*\end{array}\right] \quad (24)$$

$$\underline{z}_{stbc}[i] := \left[\begin{array}{c}\underline{z}[n]\\ \underline{z}[n+1]^*\end{array}\right] \quad (25)$$

where $i = \lfloor n/2\rfloor$. The channel and CDMA spreading matrices have been extended as given by:

$$\underline{\underline{\chi}}_{stbc} := \left[\begin{array}{c}\underline{\underline{I}}_{MN_TB}\\ \underline{\underline{I}}_M\otimes\underline{\underline{\chi}}\end{array}\right] \quad (26)$$

$$\underline{\underline{\theta}}_{stbc} := \left[\begin{array}{cc}\underline{\underline{\theta}} & \underline{\underline{0}}_{MN_TQ\times MN_TB}\\ \underline{\underline{0}}_{MN_TQ\times MN_TB} & \underline{\underline{\theta}}^*\end{array}\right] \quad (27)$$

$$\underline{\underline{H}}_{stbc} := \left[\begin{array}{cc}\underline{\underline{H}} & \underline{\underline{0}}_{N_RMQ\times MN_TQ}\\ \underline{\underline{0}}_{N_RMQ\times MN_TQ} & \underline{\underline{H}}^*\end{array}\right], \quad (28)$$

Finally, we get:

$$\underline{y}_{stbc}[i] = \underline{\underline{G}}_{stbc} \cdot \underline{d}[i] + \underline{z}_{stbc}[i] \tag{29}$$

in which the transfer matrix $\underline{\underline{G}}_{stbc}$ is the product of the channel, CDMA spreading and STBC matrices:

$$\underline{\underline{G}}_{stbc} := \underline{\underline{H}}_{stbc} \cdot \underline{\underline{\theta}}_{stbc} \cdot \underline{\underline{\chi}}_{stbc} . \tag{30}$$

IV. Receiver design

A. Multiuser joint detection

In order to detect the transmitted symbol block of the p-th user, $\underline{d}^p[i]$, based on the received sequence of blocks within the received vector, $\underline{y}_{stbc}[i]$, a first solution consists of using a single-user receiver, that inverts successively the channel and all the operations performed at the transmitter. The single-user receiver relies implicitly on the fact that CDMA spreading has been applied in addition to frequency domain equalization. However the single-user receiver fails in the uplink where multiple channels have to be inverted at the same time.

The optimal solution is to jointly detect the transmitted symbol blocks of the different users within the transmitted vector, $\underline{d}[i]$, based on the received sequence of blocks within the received vector, $\underline{y}_{stbc}[i]$. The optimum linear joint detector according to the MMSE criterion is computed in [25]. At the output of the MMSE multiuser detector, the estimate of the transmitted vector is:

$$\hat{\underline{d}}[i] = \left(\frac{\sigma_w^2}{\sigma_d^2} \underline{\underline{I}}_{MN_TB} + \underline{\underline{G}}_{stbc}^H \cdot \underline{\underline{G}}_{stbc} \right)^{-1} \cdot \underline{\underline{G}}_{stbc}^H \cdot \underline{y}_{stbc}[i] . \tag{31}$$

The MMSE linear joint detector consists of two main operations [25], [26]:

1. A filter matched to the composite impulse responses multiplies the received vector in order to minimize the impact of the white noise. The matched filter consists of the maximum ratio combining (MRC) of the different received antenna channels, the CDMA de-spreading, the STBC de-coding.
2. The output of the matched filter is still multiplied with the inverse of the composite impulse response auto-correlation matrix of size MN_TB that mitigates the remaining inter-symbol, inter-user and inter-antenna interference.

The linear MMSE receiver is different from the single-user receiver, and suffers from a higher computational complexity. Fortunately, both the initialization complexity, which is required to compute the MMSE receiver, and the data processing complexity can be significantly reduced by exploiting the initial circulant properties of the channel matrices. Based on a permutation and on the properties of the block circulant matrices given in [5], it will be shown in the next sections that the initial inversion of the square auto-correlation matrix of size MN_TB can be replaced by the inversion of B square auto-correlation matrices of size MN_T.

B. Frequency domain representation

Any block-circulant matrix can be block-diagonalized based on FFT operations. In this section, the matrix $\underline{\underline{H}} \cdot \underline{\underline{\theta}}$ is made block-circulant based on a permutation of its columns, and further block-diagonalized. As it will be shown later, this serves as a basis for the MMSE linear joint detector simplification.

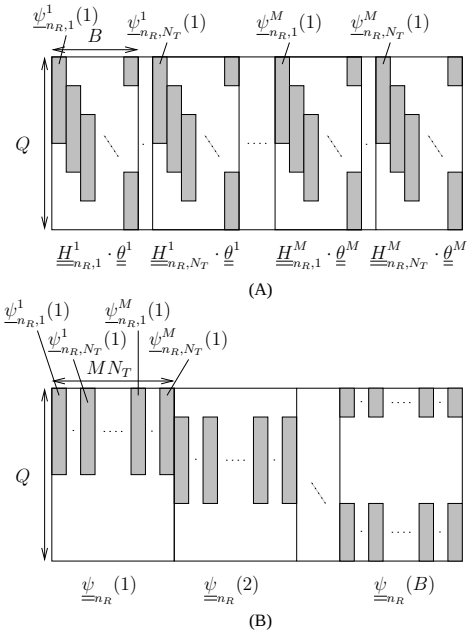

Fig. 4. (A) Initial matrix $\underline{\underline{H}}_{n_R} \cdot \underline{\underline{\theta}}$ (B) Permuted matrix $\underline{\underline{\Psi}}_{n_R}$.

The transformation of $\underline{\underline{H}} \cdot \underline{\underline{\theta}}$ is based on the special form of the user and transmit/receive antenna specific sub-matrices $\underline{\underline{\dot{H}}}^m_{n_R,n_T} \cdot \underline{\underline{\theta}}^m$. The first column $\underline{\psi}^m_{n_R,n_T}(1)$ of $\underline{\underline{\dot{H}}}^m_{n_R,n_T} \cdot \underline{\underline{\theta}}^m$ is the channel impulse response $h^m_{n_R,n_T}[l]$ convolved with the CDMA code $a^m[l]$. The b-th column $\underline{\psi}^m_{n_R,n_T}(b)$ of $\underline{\underline{\dot{H}}}^m_{n_R,n_T} \cdot \underline{\underline{\theta}}^m$ is a $(b-1)N$ cyclic rotation of the first column ($b = 1, \cdots, B$).

Considering the receive antenna n_R specific part of the $\underline{\underline{H}} \cdot \underline{\underline{\theta}}$, a permutation matrix $\underline{\underline{\Upsilon}}$ of size $MN_TB \times MN_TB$ can be defined such that (see Figure 4):

$$\underline{\underline{H}}_{n_R} \cdot \underline{\underline{\theta}} = \underline{\underline{\Psi}}_{n_R} \cdot \underline{\underline{\Upsilon}} . \tag{32}$$

The role of the matrix $\underline{\underline{\Upsilon}}$ is to reorganize the order of the columns of $\underline{\underline{H}}_{n_R} \cdot \underline{\underline{\theta}}$ according to the transmit antenna, user and symbol indexes successively (instead of symbol, transmit antenna and user indexes successively). The matrix $\underline{\underline{\Psi}}_{n_R}$ is composed of B cyclically shifted versions $\underline{\underline{\psi}}_{n_R}(b)$ of the matrix $\underline{\underline{\psi}}_{n_R}(1)$ of size $Q \times MN_T$ equal to:

$$\underline{\underline{\psi}}_{n_R}(1) := \left[\begin{array}{ccc} \underline{\underline{\psi}}^1_{n_R}(1) & \cdots & \underline{\underline{\psi}}^M_{n_R}(1) \end{array} \right] \text{ with} \tag{33}$$

$$\underline{\underline{\psi}}^m_{n_R}(1) := \left[\begin{array}{ccc} \underline{\psi}^m_{n_R,1}(1) & \cdots & \underline{\psi}^m_{n_R,N_T}(1) \end{array} \right] \tag{34}$$

for $m = 1, \cdots, M$.

The block circulant matrix $\underline{\underline{\Psi}}_{n_R}$ can be decomposed according to [5] into:

$$\underline{\underline{\Psi}}_{n_R} = \underline{\underline{F}}^H_{(N)} \cdot \underline{\underline{\Phi}}_{n_R} \cdot \underline{\underline{F}}_{(MN_T)} \tag{35}$$

where the matrices $\underline{\underline{F}}_{(N)}$ and $\underline{\underline{F}}_{(MN_T)}$ are block Fourier transforms, defined as:

$$\underline{\underline{F}}_{(n)} := \underline{\underline{F}}_B \otimes \underline{\underline{I}}_n \tag{36}$$

where $\underline{\underline{F}}_B$ is the orthogonal Fourier transform matrix of size B and $\underline{\underline{I}}_n$ is the identity matrix of size n (n equal to N or MN_T).

The block-diagonal inner matrix $\underline{\underline{\Phi}}_{n_R}$ is equal to:

$$\underline{\underline{\Phi}}_{n_R} := \begin{bmatrix} \underline{\underline{\phi}}_{n_R}(1) & \cdots & \underline{\underline{0}}_{N\times MN_T} \\ \vdots & \ddots & \vdots \\ \underline{\underline{0}}_{N\times MN_T} & \cdots & \underline{\underline{\phi}}_{n_R}(B) \end{bmatrix}, \quad (37)$$

where the block-diagonal is found by dividing the result of the product $\underline{\underline{F}}_{(N)}\,\underline{\underline{\psi}}_{n_R}(1)$ into blocks $\underline{\underline{\phi}}_{n_R}(b)$ of size $N \times MN_T$ ($b = 1, \cdots, B$).

By stacking the different receive antenna specific parts on top of each other, we get finally:

$$\underline{\underline{H}} \cdot \underline{\underline{\theta}} = (\underline{\underline{I}}_{N_R} \otimes \underline{\underline{F}}^H_{(N)}) \cdot \underline{\underline{\Phi}} \cdot \underline{\underline{F}}_{(MN_T)} \cdot \underline{\underline{\Upsilon}} \quad (38)$$

in which

$$\underline{\underline{\Phi}} := \begin{bmatrix} \underline{\underline{\Phi}}_1 \\ \vdots \\ \underline{\underline{\Phi}}_{N_R} \end{bmatrix}. \quad (39)$$

C. Receiver structure

The MMSE multi-user joint detector (31) is simplified based on the factorization (38). Taking the matrix definitions (26), (27) and (28) into account, the inner product $\underline{\underline{G}}^H_{stbc} \cdot \underline{\underline{G}}_{stbc}$ can be written as:

$$\begin{aligned} \underline{\underline{G}}^H_{stbc} \cdot \underline{\underline{G}}_{stbc} =& \underline{\underline{\Upsilon}}^H \cdot \underline{\underline{F}}^H_{(MN_T)} \cdot \underline{\underline{\Phi}}^H \cdot \underline{\underline{\Phi}} \cdot \underline{\underline{F}}_{(MN_T)} \cdot \underline{\underline{\Upsilon}} \\ &+ (\underline{\underline{I}}_M \otimes \underline{\underline{\chi}}^H) \cdot \underline{\underline{\Upsilon}}^T \cdot \underline{\underline{F}}^T_{(MN_T)} \\ &\cdot \underline{\underline{\Phi}}^T \cdot \underline{\underline{\Phi}}^* \cdot \underline{\underline{F}}^*_{(MN_T)} \cdot \underline{\underline{\Upsilon}}^* \cdot (\underline{\underline{I}}_M \otimes \underline{\underline{\chi}}) \quad (40) \\ =& \underline{\underline{\Upsilon}}^H \cdot \underline{\underline{F}}^H_{(MN_T)} \cdot (\underline{\underline{\Phi}}^H \cdot \underline{\underline{\Phi}} \\ &+ (\underline{\underline{I}}_{BM} \otimes \underline{\underline{\chi}}^*_{N_T}) \cdot \underline{\underline{\Phi}}^T \cdot \underline{\underline{\Phi}}^* \cdot (\underline{\underline{I}}_{BM} \otimes \underline{\underline{\chi}}_{N_T})) \\ &\cdot \underline{\underline{F}}_{(MN_T)} \cdot \underline{\underline{\Upsilon}}. \quad (41) \end{aligned}$$

Equality (41) has been obtained by reorganizing the STBC matrix. The matrices $\underline{\underline{\Upsilon}}$ and $\underline{\underline{F}}_{(MN_T)}$ are unitary, so that the MMSE joint detector reduces to:

$$\begin{aligned} \underline{\hat{d}}[i] =& \underline{\underline{\Upsilon}}^H \cdot \underline{\underline{F}}^H_{(MN_T)} \cdot (\frac{\sigma_w^2}{\sigma_d^2}\underline{\underline{I}}_{MN_TB} + \underline{\underline{\Phi}}^H \cdot \underline{\underline{\Phi}} \\ &+ (\underline{\underline{I}}_{BM} \otimes \underline{\underline{\chi}}^*_{N_T}) \cdot \underline{\underline{\Phi}}^T \cdot \underline{\underline{\Phi}}^* \cdot (\underline{\underline{I}}_{BM} \otimes \underline{\underline{\chi}}_{N_T}))^{-1} \\ &\cdot \begin{bmatrix} (\underline{\underline{I}}_{N_R} \otimes \underline{\underline{F}}^H_{(N)}) \cdot \underline{\underline{\Phi}} \\ (\underline{\underline{I}}_{N_R} \otimes \underline{\underline{F}}^T_{(N)}) \cdot \underline{\underline{\Phi}}^* \cdot (\underline{\underline{I}}_{N_R} \otimes \underline{\underline{\chi}}^T_{N_T}) \end{bmatrix}^H \cdot \underline{y}_{stbc}[i]\,. \end{aligned} \quad (42)$$

The inner matrix in (41) is a block diagonal matrix where each block, of size $MN_T \times MN_T$ corresponds to a symbol b. Identifying the subpart of size $N_T \times N_T$ of each block corresponding to the users m_1 and m_2, it is a diagonal matrix only if $m_1 = m_2$. *As a result of (41), the linear matched filter $\underline{\underline{G}}^H_{stbc}$ allows for optimal combining of the signals coming from the two transmit antennas and complete inter-antenna interference removal for each user independently. The high complexity inversion of the inner equalization matrix in (31) reduces to the inversion of B complex hermitian matrices of size MN_T, that will multiply the output of the matched filter in order to mitigate the remaining inter-user interference.*

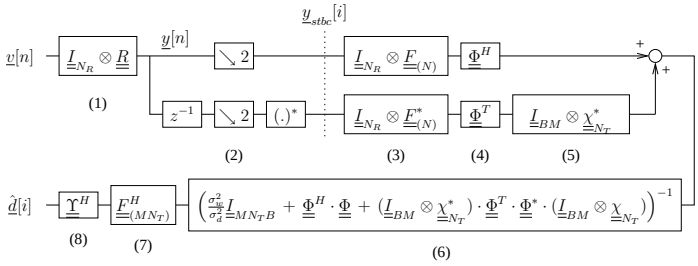

Fig. 5. Receiver.

	Time domain	Frequency domain
Inner product	$2NB^3M^3(N_RN_T)$	$2NBM^2(N_RN_T^2)$
Inversion	$2B^3M^3N_T^3$	$2BM^3N_T^3$

TABLE I
RECEIVER COMPUTATION COMPLEXITY (NUMBER OF MAC OPERATIONS).

As illustrated in Figure 5, the receiver decomposes into the successive operations:
1. CP removal
2. Separation of the two time instant streams in two STBC branches,
3. FFT for frequency domain channel equalization,
4. MRC of the different receive antenna signals and CDMA code correlation,
5. STBC decoding by combining the two successive time instants,
6. Mitigation of the inter-user interference by multiplication with the inner matrix,
7. IFFT to go back to the time domain,
8. Permutation to arrange the result according to the symbol, transmit antenna and user indexes successively.

The complexity required at the base station to compute the multiuser receiver during the initialization phase is given in Table I. The two main operations are detailed: computation of the inner matrix, inversion of the inner matrix. A significant gain of initialization complexity is achieved by computing the MMSE joint detector in the frequency domain (using the result (42)) instead of in the time domain (using the initial expression (31)).

	Time domain	Frequency domain
FFT	–	$2NN_RB\log_2 B$
Interference mitigation	$2NB^2M^2(N_RN_T)$	$2NB^2M(N_RN_T)$
IFFT	–	$MN_TB\log_2 B$

TABLE II
RECEIVE DATA PROCESSING COMPLEXITY (NUMBER OF MAC OPERATIONS PER SYMBOL BLOCK).

The complexity needed during the data processing phase to receive each transmitted complex symbol block is further given in the Table II. While additional FFT and IFFT operations are required to move to the frequency domain and to come back to the time domain, the data processing complexity required to mitigate the inter-user and inter-antenna interference is lower in the case of frequency domain processing.

V. Results

The diversity order of a multiple access channel where the users employ STBC across two transmit antennas is equal to the spatial diversity order $2N_R$ (enabled by the use of 2 transmit antennas and N_R receive antennas) times the multipath diversity order (enabled by the reception of multiple replicas of the signal through different propagation paths) as demonstrated in [27]. In this section, we evaluate how the proposed system can exploit spatial diversity and multipath diversity. The gain obtained by exploiting the spatial or multipath diversity is limited by the interference (ISI and MUI) inherent to the system. We compare the spatial diversity gain obtained under different system configurations (1 or 2 antennas at each side of the link): single-input single-output (SISO) 1x1, STBC 2x1, MRC 1x2 and STBC+MRC 2x2. The multipath diversity gain is quantified by comparing the performance obtained in case of multipath propagation to the one obtained in case of single-path propagation.

The system parameters are summarized in Table III. We consider a cellular system, which operates in an outdoor propagation environment modeled by channel model 4 of the 3GPP release 4. The channel is composed of two paths of the same amplitude and delayed by 976 ns. Each path is assumed to have a Rayleigh distribution. For mobile environments, a typical Jakes Doppler power spectrum has been assumed. The system operates at a carrier frequency of 2 GHz, with a system bandwidth of 5 MHz. The transmitted signals are shaped with a half-root Nyquist in order to limit the bandwidth. A roll-off factor equal to 0.2 has been assumed. The user signals are spread by periodic Walsh-Hadamard codes for spreading, which are overlayed with an aperiodic Gold code for scrambling. The spreading factor (SF) is equal to 8. The number of carriers is 64 and the cyclic prefix length is 16. A 16QAM constellation has been assumed. In order to not hide the spatial/multipath diversity gain by channel coding, all results are uncoded. Monte-Carlo simulations have been performed to average the bit error rate (BER) over 1000 stochastic channel realizations. The BER is determined as a function of the ratio E_b/N_0 in which E_b is the received bit energy averaged over the channels and N_0 is the one-sided noise power spectral density.

Channel model	3GPP release 4, case 4
Carrier frequency	2 GHz
Signaling rate	5 MHz
Roll-off	0.2
Spreading factor	$N = 8$
Constellation	16QAM
Number of subcarriers	$Q = 64$
Cyclic prefix length	$L = 16$
Channel code rate	uncoded

TABLE III
CELLULAR SYSTEM PARAMETERS.

Figure 6 illustrates the spatial and/or multipath diversity gain for the different system configurations when only one user is active in the system (lowest user load). Dashed curves represent the performance obtained in case of a single-path channel (no ISI, no MUI). Compared to the single-antenna system, STBC 2x1 and MRC 1x2 systems enable a spatial diversity gain of order 2. Because the BER is shown as a function of the received power, the 3 dB array gain obtained with MRC is hidden, and STBC 2x1 and MRC 1x2 perform equally well. When the two techniques are combined, the spatial diversity is of order 4. Solid curves represent the performance obtained in case of the two-path channel (ISI, no MUI). The MMSE linear joint detector succeeds in canceling most of the interference caused by the multipath channel so that the system is able to benefit also from the multipath diversity. It is observed that the single-antenna system (SISO 1x1) for a two-path channel has a performance comparable to the two-antenna systems (STBC 2x1, MRC 1x2) for a single-path channel. Therefore the SISO 1x1 system benefits fully from the multipath diversity. The gain of the multiple antenna systems (STBC 2x1, MRC 1x2, STBC+MRC 2X2) is also significant for the two-path channel compared to the single-path channel. However the remaining interference prevents the multiple antenna systems from fully benefiting from the diversity in the system (spatial and multipath) . As an example, the STBC 2x1 and MRC 1x2 systems for a two-path channel do not perform as good as the STBC+MRC 2x2 system for a single-path channel.

Figure 7 illustrates the spatial and/or multipath diversity gain for the different system configurations when 8 users are active in the system (full user load). Dashed curves represent the performance obtained in case of a single-path channel (no ISI, no MUI). Because the users are fully orthogonal (synchronous CDMA), the performance achieved with this system is exactly the same as the performance achieved by the single-user system.

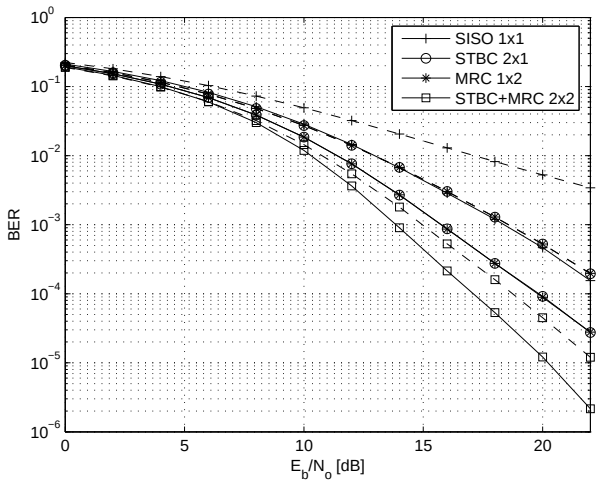

Fig. 6. Single-user system performance; dashed curves: one-path channel, solid curves: two-path channel.

Solid curves represent the performance obtained in case of the two-path channel (ISI, MUI). Due to the additional interference caused by the other users, the system is usually unable to benefit from the diversity offered by the multipath propagation. STBC 2x1 also loses a significant part of its spatial diversity gain with respect to MRC 1x2.

Figure 8 compares the performance of SC-CDMA and SCBS-CDMA [19], [20] for different user loads. In the case of a single-path channel, both systems are orthogonal in the users and perform equally well. In the case of a two-path channel, only the SCBS-CDMA system remains orthogonal in the users. When the user load is smaller than or equal to 6 users, SC-CDMA outperforms significantly SCBS-CDMA because it is better able to exploit the multipath diversity. When eight users are active in the system (full user load), the performance of SCBS-CDMA is higher than the one of SC-CDMA due to the MUI in the last system. Figure 9 further compares the performance of the two systems in a mobile environment. The BER obtained at $E_b/N_0 = 22$ dB is illustrated as a function of the terminal speed. The number of users active in the system is equal to 4 (half user load) or 8 (full user load). The symbol block duration is much higher in case of SCBS-CDMA (SF times the FFT duration, times 2 in case of STBC) than in case of SC-CDMA (FFT duration, times 2 in case of STBC). The SCBS-CDMA system is no longer orthogonal in case of time-varying channels. As a result, the performance of SCBS-CDMA is highly degraded at increasing speeds, while the performance of SC-CDMA is slightly changed. In the case of a half user load, the SC-CDMA system outperforms always the SCBS-CDMA system. In the case of a full user load, the SC-CDMA system outperforms only the SCBS-CDMA system at high speeds (higher than 120 km/h).

If there is only one user active in the system (lowest system load), STBC 2x1 and MRC 1x2 perform equally well. If there are 8 users active in the system (full system load), MRC 2x1 outperforms STBC 2x1 significantly. In case of STBC, it has been analytically proven that the inter-antenna interference of the user of interest is totally canceled out at the output of the matched filter. However, STBC still relies on the orthogonality properties of the CDMA codes and on the MMSE joint detector to handle the inter-antenna interference coming from the other users. The spatial diversity gain obtained by the use of STBC at the mobile terminals is limited by the MUI. On the contrary, MRC combines two independently faded versions of the received signal for each user without suffering from additional MUI coming from the other users. The spatial diversity gain obtained by the use of MRC combining at the base station is maximum. It is therefore interesting to investigate if more advanced receivers, capable of better compensating the MUI than the linear MMSE joint detector, would enable the STBC system to benefit also from the spatial diversity. As an example, we consider a SIC [28] built based on the linear MMSE joint detector. At each iteration, the signal of the most reliable user (in terms of estimated mean square error) is reconstructed and removed from the received signal. The process is followed until the last user is detected. The proposed SIC could be improved in many ways (remove a group of users at each step instead of only one user to trade-off complexity and performance, use soft estimates instead of detected values to reconstruct the signal...).

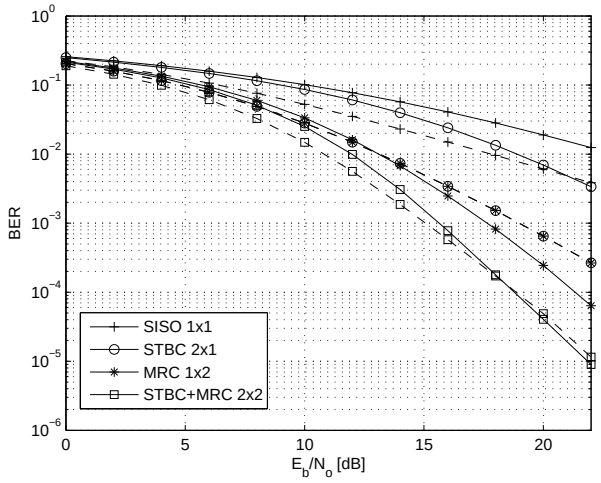

Fig. 7. Full user load system performance; dashed curves: one-path channel, solid curves: two-path channel.

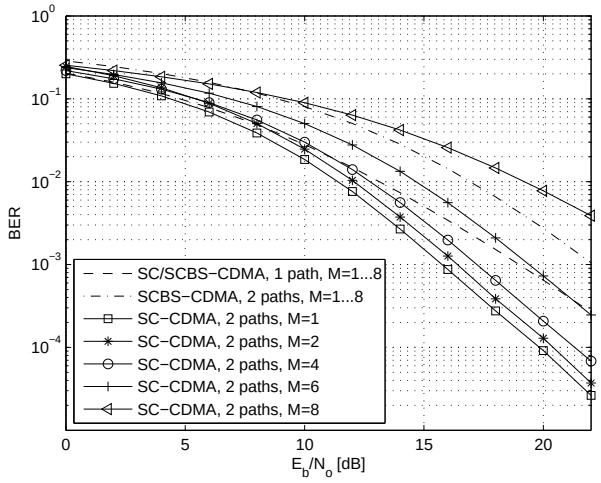

Fig. 8. Comparison SC-CDMA and SCBS-CDMA with STBC 2x1.

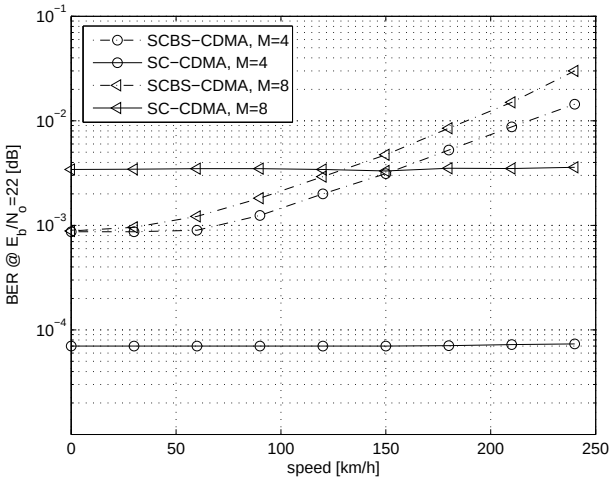

Fig. 9. Impact of the speed on SC-CDMA and on SCBS-CDMA with STBC 2x1.

However it will be shown that the proposed SIC is able to compensate the MUI very efficiently. Figure 10 illustrates the impact of the number of active users on the STBC 2x1 system performance. When a linear MMSE joint detector is used, the STBC performance moves away from the MRC performance for an increasing user load, and comes closer to the single-antenna system performance. When a SIC is used, the MUI is close to be perfectly eliminated and the performance of the 4 and 8 user systems comes very close to the one of the single user system (convergence at high SNR values). Therefore, it is shown that both spatial and multipath diversity can be exploited when advanced detection techniques are considered.

VI. Conclusion

This paper proposes a new air interface for the uplink of a cellular wireless communication system, that relies on the combination of SC-CDMA and STBC across multiple transmit antennas. The newly proposed air interface applies the STBC on the symbol blocks, before the CDMA spreading. The linear joint detector needed to mitigate the inter-user and inter-antenna interference has been derived according to the MMSE criterion. By using the cyclo-stationarity of the channels, the initialization complexity and data processing complexity of the receiver have been significantly reduced. It has been further proven that the interference between the transmit antennas is completely canceled out at the output of the joint detector. Assuming outdoor frequency selective channels, the conditions under which the proposed system is able to benefit from the spatial and multipath diversity have been studied. At low user loads, the system is capable of benefiting from the diversity. However, it has been shown that MUI is strongly destructive and prevents the system from benefiting from the diversity at high user loads. A non-linear SIC, built based on the linear MMSE joint detector, is a suitable solution to mitigate the MUI.

References

[1] T. Ojanperä and R. Prasad, *Wideband CDMA for Third Generation Mobile Communications*, Artech House Publishers, 1998.

[2] H. Sari, G. Karam, and I. Jeanclaude, "Transmission techniques for digital terrestrial TV broadcasting," *IEEE Communications Magazine*, vol. 33, no. 2, pp. 100–109, February 1995.

[3] A. Czylwik, "Comparison between adaptive OFDM and single carrier modulation with frequency domain equalization," in *IEEE Proceedings of VTC*, May 1997, pp. 865–869.

[4] D. Falconer, S.L. Ariyavisitakul, A. Benyamin-Seeyar, and B. Eidson, "Frequency domain equalization for single-carrier broadband wireless systems," *IEEE Communications Magazine*, vol. 40, no. 4, pp. 58–66, April 2002.

[5] M. Vollmer, M. Haardt, and J. Gotze, "Comparative study of joint detection techniques for TD-CDMA based mobile radio systems," *IEEE Journal on Selected Areas in Communications*, vol. 19, no. 8, pp. 1461–1475, August 2001.

[6] K.L Baum, T.A. Thomas, F.W. Vook, and V. Nangia, "Cyclic-prefix CDMA: An improved transmission method for broadband DS-CDMA cellular systems," in *IEEE Proceedings of WCNC*, March 2002, vol. 1, pp. 183–188.

[7] S. Zhou, G.B. Giannakis, and C. Le Martret, "Chip-interleaved block-spread code division multiple access," *IEEE Transactions on Communications*, vol. 50, no. 2, pp. 235–248, February 2002.

[8] F. Petré, G. Leus, L. Deneire, and M. Moonen, "Downlink frequency-domain chip equalization for single-carrier block transmission DS-CDMA with known symbol padding," in *IEEE Proceedings of Globecom*, November 2002, vol. 1, pp. 453–457.

[9] N. Yee, J-P. Linnartz, and G. Fettweis, "Multicarrier CDMA in indoor wireless radio networks," in *IEEE Proceedings of PIMRC*, September 1993, vol. 1, pp. 109–113.

[10] K. Fazel, "Performance of CDMA/OFDM for mobile communication system," in *IEEE Proceedings of ICUPC*, October 1993, vol. 2, pp. 975–979.

[11] V.M. DaSilva and E.S. Sousa, "Multicarrier orthogonal CDMA signals for quasi-synchronous communication systems," *IEEE Journal on Selected Areas in Communications*, vol. 12, no. 5, pp. 842–852, June 1994.

[12] S. Kondo and L.B. Milstein, "Performance of multicarrier DS-CDMA systems," *IEEE Transactions on Communications*, vol. 44, no. 2, pp. 238–246, February 1996.

[13] F. Petré, G. Leus, M. Moonen, and H. De Man, "Multi-carrier block-spread CDMA for broadband cellular downlink," *EURASIP Journal on Applied Signal Processing, Special issue on Multi-Carrier Communications and Signal Processing*, vol. 2004, no. 10, August 2004.

[14] F. Horlin, F. Petre, E. Lopez, F. Naessens, and L. Van der Perre, "Flexible transmission scheme for 4G wireless systems with multiple antennas," *Eurasip JWCN, special issue on Reconfigurable Radio for Future Generation Wireless Systems*, , no. 3, pp. 308–322, August 2005.

[15] S. M. Alamouti, "A simple transmit diversity technique for wireless communications," *IEEE Journal on Selected Areas in Communications*, vol. 16, no. 8, pp. 1451–1458, October 1998.

[16] V. Tarokh, H. Jafarkhani, and A. R. Calderbank, "Space-time block codes from orthogonal designs," *IEEE Transactions on Information Theory*, vol. 45, pp. 1456–1467, July 1999.

[17] E. Lindskog and A. Paulraj, "A transmit diversity scheme for channels with intersymbol interference," in *IEEE Proceedings of ICC*, June 2000, vol. 1, pp. 307–311.

[18] G. Ganesan and P. Stoica, "Space-time block codes: A maximum SNR approach," *IEEE Transactions on Information Theory*, vol. 47, pp. 1650–1656, May 2001.

[19] F. Petré, G. Leus, L. Deneire, M. Engels, M. Moonen, and H. De Man, "Space-time block-coding for single-carrier block-transmission DS-CDMA downlink," *IEEE Journal on Selected Areas in Communications, Special issue on MIMO Systems and Applications*, vol. 21, no. 3, pp. 350–361, April 2003.

[20] K. C. B. Wavegedara, D. V. Djonin, and V. K. Bhargava, "Space-time-coded CDMA uplink transmission with MUI-free reception," *IEEE Transactions on Wireless Communications*, vol. 4, no. 6, pp. 3095–3105, November 2005.

[21] S. Barbarossa and F. Cerquetti, "Simple space-time coded SS-CDMA systems capable of perfect MUI/ISI elimination," *IEEE Communications Letters*, vol. 5, no. 12, pp. 471–473, December 2001.

[22] F. W. Vook, T. A. Thomas, and K. L. Baum, "Cyclic-prefix CDMA with antenna diversity," in *IEEE Proceedings of VTC-Spring*, May 2002, vol. 2, pp. 1002–1006.

[23] K. Takeda and F. Adachi, "MMSE frequency-domain equalization combined with space-time transmit diversity and antenna receive diversity for DS-CDMA," in *IEEE Proceedings of VTC-Spring*, May 2004, vol. 1, pp. 464–468.

[24] Z. Wang and G.B. Giannakis, "Wireless multicarrier communications: Where Fourier meets Shannon," *IEEE Signal Processing Magazine*, vol. 17, no. 3, pp. 29–48, May 2000.

[25] A. Klein, G.K. Kaleh, and P.W. Baier, "Zero forcing and minimum mean-square-error equalization for multiuser detection in code-division

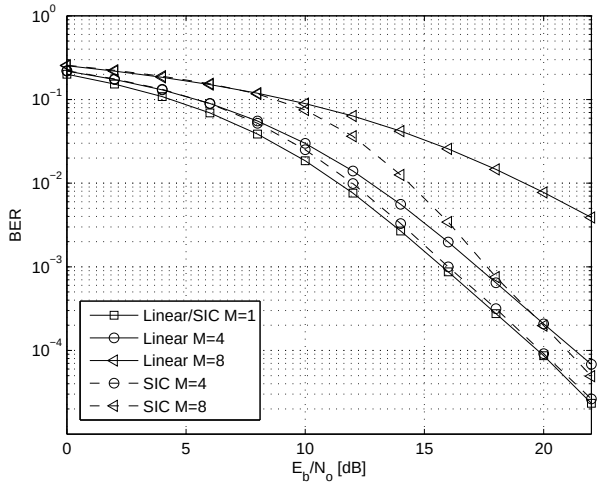

Fig. 10. Impact of user load on SC-CDMA with STBC 2x1. Comparison of the linear MMSE joint detector and the SIC performances.

multiple-access channels," *IEEE Transactions on Vehicular Technology*, vol. 14, no. 9, pp. 1784–1795, December 1996.

[26] L. Vandendorpe, "Performance analysis of IIR and FIR linear and decision-feedback mimo equalizers for transmultiplexers," in *IEEE Proceedings of ICC*, June 1997, vol. 2, pp. 657–661.

[27] S. N. Diggavi, N. Al-Dhahir, and A. R. Calderbank, "Algebraic properties of space-time block codes in intersymbol interference multiple-access channels," *IEEE Transactions on Information Theory*, vol. 49, no. 10, pp. 2403–2414, October 2003.

[28] N. Benvenuto and P. Bisaglia, "Parallel and successive interference cancellation for MC-CDMA and their near-far resistance," in *IEEE Proceedings of VTC-Fall*, October 2003, vol. 2, pp. 1045–1049.